CrystEngComm

COMMUNICATION

View Article Online
View Journal | View Issue

Check for updates

Cite this: *CrystEngComm*, 2020, **22**, 425

Received 25th October 2019,
Accepted 14th December 2019

DOI: 10.1039/c9ce01698h

rsc.li/crystengcomm

Polymorphs of a copper coordination compound: interlinking active sites enhance the electrocatalytic activity of the coordination polymer compared to the coordination complex†

Pandi Muthukumar,[a] Mehboobali Pannipara,[bc] Abdullah G. Al-Sehemi,[bc] Dohyun Moon*[d] and Savarimuthu Philip Anthony*[a]

Copper–pyridinedicarboxylic acid produces concomitant polymorphs, a copper complex (Cu–C) and a coordination polymer (Cu–P), which have a similar coordination environment but completely different electrocatalytic activity. Cu–P displayed highly enhanced activity for the hydrogen evolution reaction (HER, η@10 mA cm^{-2} = 285 mV, j_{max} = 161.7 mA cm^{-2}) compared to Cu–C (η@10 mA cm^{-2} = 444 mV, j_{max} = 48.7 mA cm^{-2}) in a neutral medium.

Metal coordination complexes and polymers with intriguing structural topologies have received significant attention in the last few decades because of their promising application potential in various fields, including catalysis, gas storage/separation, bio-imaging and energy storage.[1,2] The versatility of the ligand coordination and metal coordination geometry allows network structures to be engineered with the desired topology, functionality, porosity and uncoordinated metal sites for achieving enhanced material properties. Metal complexes and coordination polymers have been extensively used as homogeneous/heterogeneous catalysts for organic chemical transformations and energy production.[3] However, the direct comparison of the catalytic activity of the same metal complex and coordination polymer with a similar coordination environment has never been studied due to the synthetic difficulty; however, this will provide structural insight for the fabrication of efficient catalysts.

In recent years, there has been a strong search for sustainable alternative energy sources to traditional fossil fuels due to the ever increasing energy demand and environmental concern.[4] Hydrogen (H_2), with highest mass energy density and clean combustion with air, is considered a future green energy source.[5] Electrochemical water splitting is one of the cleanest and most sustainable methods for producing H_2 to meet future energy demands.[6] However, highly active and robust electrocatalysts are required to minimize the energy barrier, which is the overpotential (η), of the water splitting process for the efficient generation of H_2.[7] To date, the noble metal platinum (Pt) catalyst is the best HER electrocatalyst, but its scarcity and high cost limit its practical applications.[8] The earth-abundant transition metals with multiple oxidation states are potential alternatives for developing efficient and highly stable non-noble electrocatalysts.[9,10] Most of these catalysts show strong HER activity in acidic medium; however, neutral or alkaline medium efficient HER electrocatalysts are preferable for practical applications due to environmental problems and the corrosive nature of acidic media. However, the additional step, water dissociation, involved in the HER mechanism in alkaline or neutral medium requires a higher overpotential with transition metal catalyst and also with platinum-group metal catalysts.[11]

Thus, the use of coordination complexes and polymers as electrocatalysts for the HER has attracted significant attention in recent years because of their tailorable structure.[12] Cobalt corrole is the first molecular complex reported to exhibit HER activity across a wide pH range.[13] Similarly, there is a limited number of metal coordination polymers that show strong HER electrocatalytic activities.[14] However, these electrocatalysts require complimentary conducting materials such as graphene oxide and acetylene black to enhance their conducting property and electrocatalytic activities.[15] For example, cobalt and nickel ions were immobilised on 2D conjugated dithiolene ligands

---

[a] *Department of Chemistry, School of Chemical & Biotechnology, SASTRA Deemed University, Thanjavur-613401, Tamil Nadu, India.*
E-mail: philip@biotech.sastra.edu
[b] *Department of Chemistry, King Khalid University, Abha 61413, Saudi Arabia*
[c] *Research center for Advanced Materials Science, King Khalid University, Abha 61413, Saudi Arabia*
[d] *Beamline Department, Pohang Accelerator Laboratory, 80 Jigokro-127beongil, Nam-gu, Pohang, Gyeongbuk, Korea. E-mail: dmoon@postech.ac.kr*

† Electronic supplementary information (ESI) available: Electrochemical studies, thermogravimetric data, PXRD, single crystal data (CCDC no. 1936561) and molecular packing. For ESI and crystallographic data in CIF or other electronic format see DOI: 10.1039/c9ce01698h

to improve their conductivity and HER activity.[16] Plasma etching of cobalt coordination polymers generates more unsaturated metal sites, which lead to enhanced electrocatalytic activity.[17] Our group has been exploring earth-abundant copper-based materials for the development of efficient electrocatalysts.[18a–c] Recently, we reported the synthesis of copper coordination polymer/complexes based on pyridine carboxylic acid with different structural motifs and water coordination-controlled HER activity in a neutral medium without the addition of any complimentary additive components.[18] During our investigation on the formation of copper coordination polymer/complexes under different conditions, we observed the formation of two different coloured crystals in aqueous medium at room temperature in the presence of DABCO base. In this study, we report concomitant polymorphic structures, a copper complex (Cu–C) and copper coordination polymer (Cu–P), and their structure-dependent HER activity in neutral (1.0 M PBS, pH = 7.0) and alkaline media (1.0 M KOH, pH = 14.0). Interestingly, both Cu–C and Cu–P exhibit similar coordination environments around the copper metal centre and differ only in their network structure. In contrast, Cu–P exhibits highly enhanced HER activity compared to Cu–C. Cu–P requires a low overpotential (η = 285 mV) to produce a geometric current density of 10 mA cm^{-2} in neutral medium compared to Cu–C (η = 444 mV). Moreover, strong HER activity was observed without the addition of any complimentary conducting materials. Both Cu–C and Cu–P displayed similar trends in an alkaline medium, but they also required higher overpotential to produce 10 mA cm^{-2}. The present work indicates that metal coordination polymers with appropriate coordination environment can exhibit strong electrocatalytic activity in neutral and alkaline media.

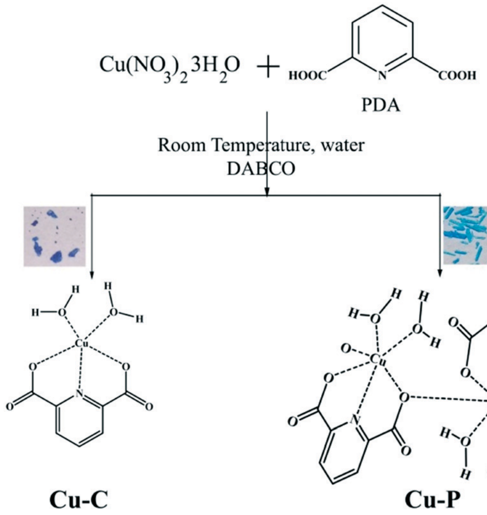

Scheme 1 Schematic of the synthesis of the Cu–C and Cu–P concomitant polymorphs. Digital images and coordination network in Cu–C and Cu–P are also shown.

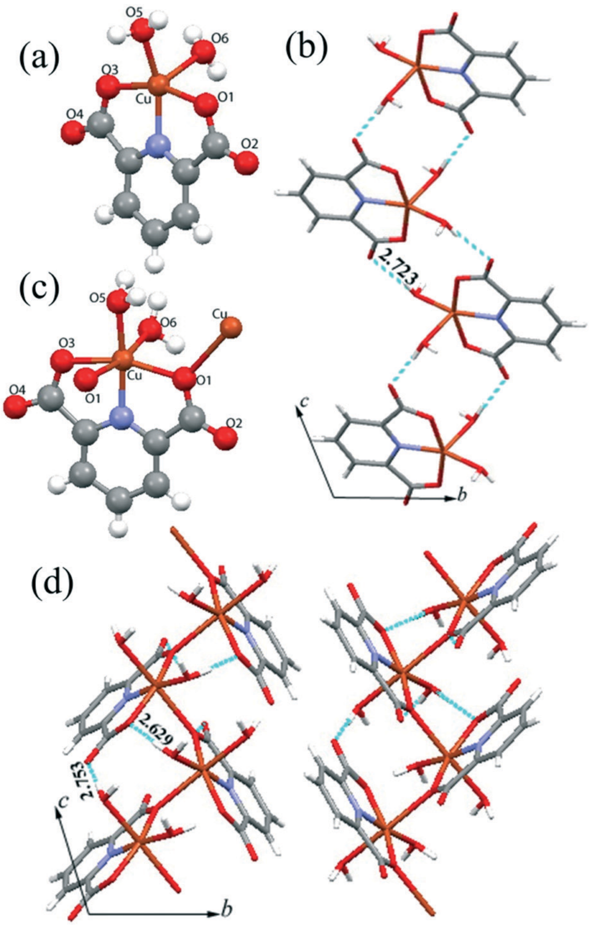

Fig. 1 Different coordination geometries and H-bonding interactions in the crystal lattice of (a and b) Cu–C and (c and d) Cu–P. C (grey), N (blue), O (red), H (white) and Cu (orange). H-Bonds (broken line). $d_{D\cdots A}$ distances are marked (Å).

In our previous work, copper and 2,6-pyridinecarboxylic acid (PDA) were dissolved in DMF in the presence of different organic bases and treated hydrothermally or kept at room temperature to produce copper coordination polymer/complexes with varying coordination geometries and structures.[18c,d] When copper nitrate, PDA and DABCO were dissolved in water and left undisturbed at room temperature, blue and cyan concomitant polymorphic crystals were formed after a few days (Scheme 1). The single crystal analysis confirmed the polymorphic structures of the copper complex (blue crystals, Cu–C) and the coordination polymer (cyan crystals, Cu–P). The copper in Cu–C adopted a square pyramidal coordination geometry *via* tridentate coordination from the PDA ligand and two water molecules (Fig. 1a and S1†). Cu–C perfectly matches the reported structure (CCDC no. 139881). Strong intermolecular H-bonding between the PDA carbonyl oxygen and coordinated water connects the molecules along the *c*-axis (Fig. 1b). In contrast, the copper in Cu–P adopts an octahedral coordination geometry, and forms four coordination bonds with the PDA ligand and coordination bonds with two water molecules (Fig. 1c and S1†). One of the carboxylate oxygen atoms (O1) of the PDA ligand coordinates to two copper centres in Cu–P to produce a 1D coordination polymeric network structure (Fig. 1d). Cu–C and Cu–P show nearly similar bond lengths except for the bond bridging oxygen and copper, which exhibited a slightly higher bond length (Fig. S2†). Cu–P also exhibited strong intermolecular H-bonding between the coordinated water and PDA carboxylate oxygen (Fig. 1d). Although their coordination geometry is different, typically, both Cu–C and Cu–P exhibit a similar coordination environment of one PDA ligand and two water molecules. The carboxylate oxygen bridging coordination in Cu–P produces a coordination polymer with an octahedral metal centre. Thermogravimetric analysis (TGA) of Cu–C did not show a clear loss of water molecules before decomposing at 180 °C (Fig. S3a†). In contrast, Cu–P showed the loss of both water molecules at 180 °C and decomposed at 280 °C (Fig. S3b†). The digital images of the Cu–C and Cu–P samples heated at 210 °C visibly showed the decomposition of Cu–C, but no significant colour change for Cu–P (Fig. S4†). Thus, the concomitant polymorphs were physically separated since they exhibited visibly different colours.

The phase purity of Cu–C and Cu–P was confirmed by powder X-ray diffraction (PXRD), which showed the perfect matching of the experimental pattern with the simulated patterns (Fig. S5†). Their similar coordination environment but complex and coordination polymeric network structure provides the opportunity to correlate the electrocatalytic activity between the complex and coordination polymer.

Both Cu–C and Cu–P exhibited good stability in alkaline, neutral and acidic media (Fig. S6†). Their stability was confirmed by immersing solids of Cu–C and Cu–P in different media for 1 h and measuring their absorption spectrum, which did not show any peak corresponding to Cu^{2+} ions. The electrocatalytic HER activities of glassy carbon electrodes modified using Cu–C and Cu–P were studied by performing electrochemical experiments in alkaline (pH = 14.0, 1.0 M KOH) and neutral media (pH = 7.0, 1.0 M PBS) at a scan rate of 50 mV s^{-1}. The electrode with glassy carbon showed poor HER activity, whereas Pt/C (20 wt%) exhibited strong activity with a very low overpotential (η) and high current density (j). Cu–C and Cu–P showed structure-dependent HER activity both in alkaline and neutral media, as shown in Fig. 2. In alkaline condition, Cu–C showed the current density of 84.8 mA cm^{-2} at the applied potential of 720 mV (Fig. 2a). In contrast, the coordination polymer, Cu–P, showed a higher current density of 129.2 mA cm^{-2} at the same applied potential. To achieve the geometric current density of 10 mA cm^{-2}, the Cu–C complex catalyst required an overpotential of 537 mV, whereas the Cu–P coordination polymer catalyst required an overpotential of 455 mV. The Tafel slope for Cu–C, Cu–P and commercial Pt/C in alkaline medium is shown in Fig. 2b. Cu–P exhibited a relatively lower Tafel slope (89 mV dec^{-1}) compared to that of Cu–C (108 mV dec^{-1}). The comparison of the current density, overpotential @10 mA cm^{-2} and Tafel slope indicates that Cu–P exhibited clearly better HER catalytic activity compared to that of Cu–C.

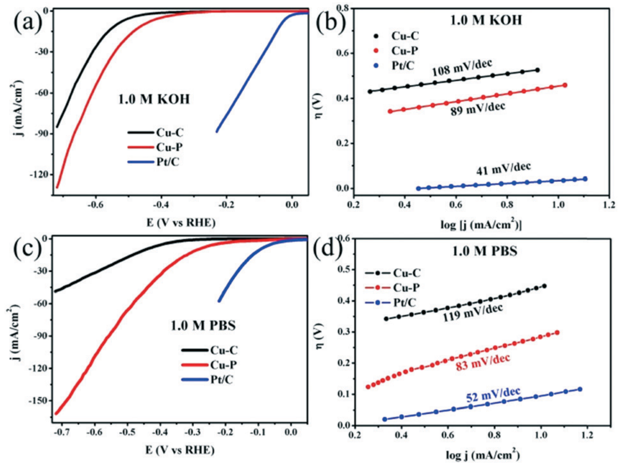

Fig. 2 HER polarization curves and Tafel plots of Cu–C and Cu–P in (a and b) 1.0 M KOH and (c and d) 1.0 M PBS, respectively.

Interestingly, the HER electrocatalytic studies of Cu–C and Cu–P in neutral medium (pH = 7.0, 1.0 M PBS) revealed drastically enhanced activity for Cu–P with a large difference between the complex and coordination polymer (Fig. 2c). Cu–P showed a current density of 161.7 mA cm^{-2} at the applied potential (720 mV), which is nearly four times higher than that of Cu–C (48.7 mA cm^{-2}). It was noted that current density of Cu–P was enhanced, whereas that of Cu–C was reduced in neutral medium. Importantly, the geometric current density of 10 mA cm^{-2} was achieved using the Cu–P catalyst with a low overpotential of 285 mV. In contrast, the Cu–C electrocatalyst required an overpotential of 444 mV to produce the geometric current density of 10 mA cm^{-2}. However, although Cu–C produced a lower current density in neutral medium compared to alkaline, it required a lower potential to produce 10 mA cm^{-2} in neutral medium. It is worthy to note that the overpotential of Cu–P is the lowest overpotential reported to date for any coordination polymer, metal–organic framework or complex without the addition of complimentary conducting materials (Tables S1 and S2†). Most importantly, the Cu–P catalyst required lowest overpotential @10 mA cm^{-2} and exhibited a high current response in neutral medium. All the reported coordination polymer-based electrocatalysts exhibited strong HER activity only after the addition of complementary conducting materials and also in acidic medium. It is noted that our previously reported water coordinated copper–PDA coordination polymer required 290 mV to achieve 10 mA cm^{-2} and produced a current density of 85 mA cm^{-2} at the applied potential of 730 mV.[18c] Cu–P showed a two times higher current density (161.7 mA cm^{-2}@720 mV). To confirm the reproducibility, the Cu–C and Cu–P HER activity in alkaline and neutral medium was repeated twice using different batches of samples (Fig. S7†). Cu–P showed a relatively lower Tafel slope (83 mV dec^{-1}) compared to that of Cu–C of 119 mV dec^{-1} (Fig. 2d). The Tafel slope of the highly active Cu–P (83 mV dec^{-1}) did not match the rate determining step of the Tafel (30 mV dec^{-1}), Heyrovsky (40 mV dec^{-1}) and Volmer (120 mV dec^{-1}) reaction mechanisms. Hence, the Tafel slope value suggests that multiple chemical reactions, *i.e.*, the Volmer–Heyrovsky mechanism, may be involved in the electrode-catalyst interface during the HER. This also further suggests that the desorption process (Volmer reaction) may be the rate-determining step followed by the faster Heyrovsky desorption process.[19] Water-coordinated cobalt coordination polymers have been reported to exhibit enhanced HER activity in acidic conditions due to the H-bonding ability of coordinated water compared to non-water coordinated cobalt coordination polymers.[15] Interestingly, two water molecules are coordinated in both Cu–C and Cu–P, but Cu–P displayed strongly enhanced HER activity compared to Cu–C. Hence, these results indicate that not only the water coordination, but the structural framework also plays an important role in the catalytic activity. The reason for the strongly enhanced activity for the coordination polymer compared to the complex may be due to the exposure of more active sites *via* extended coordination-induced structural rigidification (Scheme 2). The ability of copper to display multiple oxidation states (Cu^{1+} and Cu^{2+}) has been exploited for electrocatalytic activity.[14] The single crystal structural analysis confirmed Cu^{2+} in both Cu–C and Cu–P. Hence, during the electrocatalytic reaction, it may undergo a reversible oxidation state change between Cu^{2+} and Cu^{1+}. The FE-SEM images of the crushed Cu–P and Cu–C show they maintained rod and plate morphologies, respectively (Fig. S9†).

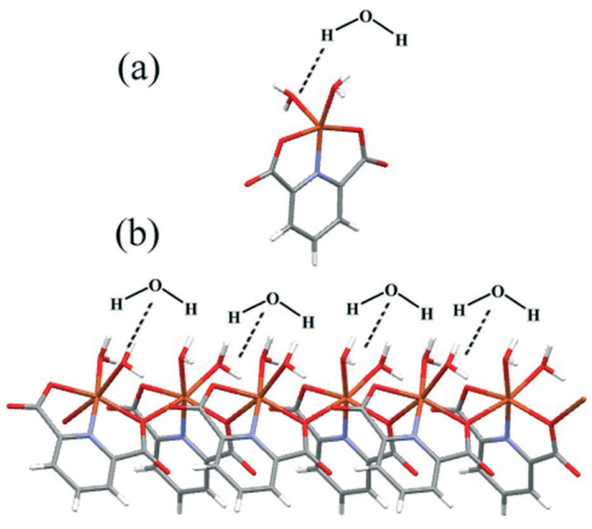

Scheme 2 Schematic representation of the increased water molecule interaction in (b) Cu–P compared to (a) Cu–C. C (grey), N (blue), O (red), H (white) and Cu (orange).

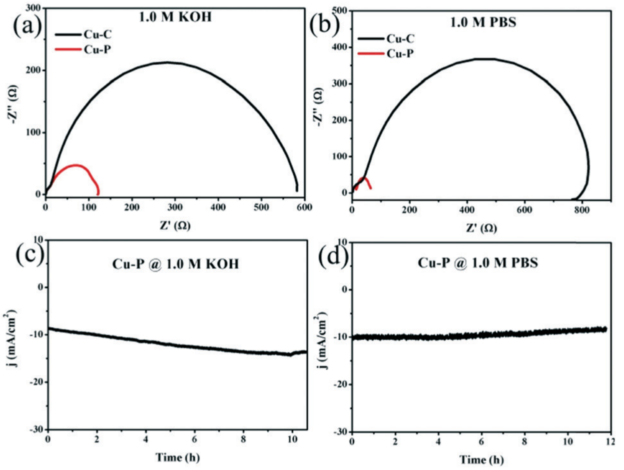

Fig. 3 Electrochemical impedance spectra (EIS) of Cu–C and Cu–P in (a) 1.0 M KOH and (b) 1.0 M PBS and current–time chronoamperometric response of Cu–P in (c) 1.0 M KOH and (d) 1.0 M PBS.

The electrochemical impedance spectra (EIS) of the Cu–C and Cu–P catalysts were measured to gain insight into their electrode kinetics (Fig. 3a and b, respectively). The impedance plots of both Cu–C and Cu–P are composed of a semicircle in the high frequency regions and a vertical line in the low frequency regions. The charge-transfer resistance is clearly different for both Cu–C and Cu–P. Cu–P exhibited a much lower charge-transfer resistance in both alkaline and neutral media compared to Cu–C. The very low charge-transfer resistance suggests highly efficient electron transfer and favorable HER kinetics at the Cu–P electrolyte interface. Stability, a very important parameter for practical applications, was monitored for the highly active Cu–P catalyst in both alkaline and acidic media (Fig. 3c and d, respectively). Although Cu–P showed a decrease in current density with time in alkaline medium, a stable and steady current density was observed in neutral medium for more than 10 h. Furthermore, the initial and 1000th cycle for Cu–P in neutral medium did not show any change, whereas a slight reduction activity was observed in alkaline medium (Fig. S8†). Although, both Cu–C and Cu–P showed good stability in acidic medium, the HER studies using 0.5 M H_2SO_4 revealed significantly reduced activity (Fig. S10†).

In conclusion, a polymorphic copper coordination complex (Cu–C) and polymer (Cu–P) with a similar coordination environment were synthesised, and the effect of their structural difference on their electrocatalytic activity was demonstrated. Cu–P exhibited higher electrocatalytic HER activity compared to that of Cu–C both in alkaline and neutral media. Importantly, Cu–P displayed a drastically enhanced current density (161.7 mA cm^{-2}) compared to that of Cu–C (48.7 mA cm^{-2}) at the applied potential and required a low overpotential (285 mV) to produce the geometric current density (10 mA cm^{-2}). The Cu–P catalyst exhibited good stability without significant loss in activity. The Tafel slope and impedance studies further supported its enhanced activity. Overall, the comparison of the copper coordination polymer electrocatalysts clearly indicates that coordination polymers with water coordination are better catalysts compared to complexes.

Financial support from the Nanomission, Department of Science and Technology, New Delhi, India (DST-Nanomission scheme no. SR/NM/NS-1053/2015) is acknowledged with gratitude. The Deanship of Scientific Research at King Khalid University is greatly appreciated for funding (R.G.P.2/48/40).

The CRF facility of SASTRA University is also acknowledged for absorption spectroscopy. X-ray crystallography at the PLS-II 2D-SMC beamline was supported in part by MSIP and POSTECH. We thank Dr. P. Suresh Kumar for use of his lab electrochemical facility.

Conflicts of interest

There are no conflicts to declare.

Notes and references

1 (*a*) S. Liu, L. Sun, F. Xu, J. Zhang, C. Jiao, F. Li, Z. Li, S. Wang, Z. Wang, X. Jiang, H. Zhou, L. Yang and C. Schick, *Energy Environ. Sci.*, 2013, **6**, 818; (*b*) Z. Zhang, Y. Zhao, Q. Gong, Z. Li and J. Li, *Chem. Commun.*, 2013, **49**, 653; (*c*) J. Della Rocca, D. Liu and W. Lin, *Acc. Chem. Res.*, 2011, **44**, 957; (*d*) Z. Hu, B. J. Deibert and J. Li, *Chem. Soc. Rev.*, 2014, **43**, 5815; (*e*) Y. Zhao, Z. Song, X. Li, Q. Sun, N. Cheng, S. Lawes and X. Sun, *Energy Storage Mater.*, 2016, **2**, 35.

2 (*a*) A. J. Amali, J.-K. Sun and Q. Xu, *Chem. Commun.*, 2014, **50**, 1519; (*b*) W. L. Leong and J. J. Vittal, *Chem. Rev.*, 2011, **111**, 688; (*c*) J. Chen, Y. Zhang, H. Ye, J.-Q. Xie, Y. Li, C. Yan, R. Sun and C.-P. Wong, *ACS Appl. Energy Mater.*, 2019, **2**, 2734.

3 (*a*) E. Loukopoulos and G. E. Kostakis, *J. Coord. Chem.*, 2018, **71**, 371; (*b*) J. Zhou and B. Wang, *Chem. Soc. Rev.*, 2017, **46**, 6927; (*c*) C. Tsay and J. Y. Yang, *J. Am. Chem. Soc.*, 2016, **138**, 4174; (*d*) S. C. Eady, M. M. MacInnes and N. Lehnert, *Inorg. Chem.*, 2017, **56**, 11654.

4 (*a*) Q. Liu, J. Tian, W. Cui, P. Jiang, N. Cheng, A. M. Asiri and X. Sun, *Angew. Chem., Int. Ed.*, 2014, **53**, 6710; (*b*) F. Lyu, Q. Wang, S. M. Choi and Y. Yin, *Small*, 2018, 1804201.

5 (*a*) L. Chen, X. Dong, Y. Wang and Y. Xia, *Nat. Commun.*, 2016, **7**, 11741; (*b*) Y. Wang, D. Yan, S. El Hankari, Y. Zou and S. Wang, *Adv. Sci.*, 2018, **5**, 1800064.

6 (*a*) N. S. Lewis and D. G. Nocera, *Proc. Natl. Acad. Sci. U. S. A.*, 2006, **103**, 15729; (*b*) J. Luo, J.-H. Im, M. T. Mayer, M. Schreier, M. K. Nazeeruddin, N.-G. Park, S. D. Tilley, H. J. Fan and M. Grätzel, *Science*, 2014, **345**, 1593.

7 (*a*) J. Zhang, J. Wu, X. Zou, K. Hackenberg, W. Zhou, W. Chen, J. Yuan, K. Keyshar, G. Gupta, A. Mohite, P. M. Ajayan and J. Lou, *Mater. Today*, 2019, **25**, 28; (*b*) Y. Zhu, H.-C. Chen, C.-S. Hsu, T.-S. Lin, C.-J. Chang, S.-C. Chang, L.-D. Tsai and H. M. Chen, *ACS Energy Lett.*, 2019, **4**, 987; (*c*) Z. Kang, H. Guo, J. Wu, X. Sun, Z. Zhang, Q. Liao, S. Zhang, H. Si, P. Wu, L. Wang and Y. Zhang, *Adv. Funct. Mater.*, 2019, **29**, 1807031.

8 C. C. L. McCrory, S. Jung, I. M. Ferrer, S. M. Chatman, J. C. Peters and T. F. Jaramillo, *J. Am. Chem. Soc.*, 2015, **137**, 4347.

9 (*a*) X. Liu, S. Cui, Z. Sun and P. Du, *Chem. Commun.*, 2015, **51**, 12954; (*b*) H. Hu, Q. Zhang, F. Luo, L. Guo, K. Qu, Z. Yang, S. Xiao, Z. Xu, W. Cai and H. Cheng, *ChemElectroChem*, 2019, **6**, 1413.

10 (*a*) Y. Wang, M. Qiao, Y. Li and S. Wang, *Small*, 2018, **14**, 1800136; (*b*) A. Han, H. Zhang, R. Yuan, H. Ji and P. Du, *ACS Appl. Mater. Interfaces*, 2017, **9**, 2240; (*c*) S. K. Kim, Y. Qiu, Y.-J. Zhang, R. Hurt and A. Peterson, *Appl. Catal., B*, 2018, **235**, 36.

11 N. Mahmood, Y. Yao, J.-W. Zhang, L. Pan, X. Zhang and J.-J. Zou, *Adv. Sci.*, 2018, **5**, 1700464.

12 (*a*) S. Elmas, T. J. Macdonald, W. Skinner, M. Andersson and T. Nann, *Polymer*, 2019, **11**, 110; (*b*) C. Xu, H. Wang, Q. Wang, Y. Wang, Y. Zhang and G. Fan, *Appl. Surf. Sci.*, 2019, **466**, 193; (*c*) B. Zhou, J. Zheng, J. Duan, C. Hou, Y. Wang, W. Jin and Q. Xu, *ACS Appl. Mater. Interfaces*, 2019, **11**, 21086.

13 (*a*) H. Sun, Y. Han, H. Lei, M. Chen and R. Cao, *Chem. Commun.*, 2017, **53**, 6195; (*b*) X. Li, H. Lei, J. Liu, X. Zhao, S. Ding, Z. Zhang, X. Tao, W. Zhang, W. Wang, X. Zheng and R. Cao, *Angew. Chem., Int. Ed.*, 2018, **57**, 15070.

14 (*a*) M. Jahan, Z. Liu and K. P. Loh, *Adv. Funct. Mater.*, 2013, **23**, 5363; (*b*) X. Wang, W. Zhou, Y.-P. Wu, J.-W. Tian, X.-K. Wang, D.-D. Huang, J. Zhao and D.-S. Li, *J. Alloys Compd.*, 2018, **753**, 228.

15 (*a*) W. Zhou, Y.-P. Wu, X. Wang, J.-W. Tian, D.-D. Huang, J. Zhao, Y.-Q. Lan and D.-S. Li, *CrystEngComm*, 2018, **20**, 4804; (*b*) Y.-P. Wu, W. Zhou, J. Zhao, W.-W. Dong, Y.-Q. Lan, D.-S. Li, C. Sun and X. Bu, *Angew. Chem., Int. Ed.*, 2017, **56**, 13001; (*c*) J.-W. Tian, M.-X. Fu, D.-D. Huang, X.-K. Wang, Y.-P. Wu, J. Y. Lu and D.-S. Li, *Inorg. Chem. Commun.*, 2018, **95**, 73.

16 (*a*) R. Dong, Z. Zheng, D. C. Tranca, J. Zhang, N. Chandrasekhar, S. Liu, X. Zhuang, G. Seifert and X. Feng, *Chem. – Eur. J.*, 2017, **23**, 2255; (*b*) S. C. Eady, M. M. MacInnes and N. Lehnert, *Inorg. Chem.*, 2017, **56**, 11654; (*c*) C. A. Downes, A. J. Clough, K. Chen, J. W. Yoo and S. C. Marinescu, *ACS Appl. Mater. Interfaces*, 2018, **10**, 1719.

17 D. Yan, C.-L. Dong, Y.-C. Huang, Y. Zou, C. Xie, Y. Wang, Y. Zhang, D. Liu, S. Shen and S. Wang, *J. Mater. Chem. A*, 2017, **6**, 805.

18 (*a*) P. Muthukumar, V. V. Kumar, G. R. K. Reddy, P. S. Kumar and S. P. Anthony, *Catal. Sci. Technol.*, 2018, **8**, 1414; (*b*) P. Muthukumar, P. S. Kumar and S. P. Anthony, *Mater. Res. Express*, 2019, **6**, 025518; (*c*) P. Muthukumar, D. Moon and S. P. Anthony, *Catal. Sci. Technol.*, 2019, **9**, 4347; (*d*) M. Koman, J. Moncol, D. Hudecová, B. Dudová, M. Melnik, M. Korabik and J. Mroziński, *Pol. J. Chem.*, 2001, **75**, 957.

19 W. F. Chen, S. Iyer, S. S. Iyer, K. Sasaki, C. H. Wang, Y. Zhu, J. T. Muckerman and E. Fujita, *Energy Environ. Sci.*, 2013, **6**, 1818.